ACS Catalysis

pubs.acs.org/acscatalysis | Letter

Nature and Reactivity of Oxygen Species on/in Silver Catalysts during Ethylene Oxidation

Tiancheng Pu,[∥] Adhika Setiawan,[∥] Bar Mosevitzky Lis,[∥] Minghui Zhu, Michael E. Ford, Srinivas Rangarajan,* and Israel E. Wachs*

Cite This: *ACS Catal.* 2022, 12, 4375−4381 | Read Online

ACCESS | Metrics & More | Article Recommendations | Supporting Information

ABSTRACT: The nature of surface oxygen species on/in a silver powder catalyst and their reactivity with ethylene were systematically investigated with multiple spectroscopies and DFT calculations. Unique quasi *in situ* HS-LEIS, *in situ* NAP-XPS, and *in situ* Raman spectroscopy demonstrated that the silver surface is covered by a thin oxide layer (1−3 nm) after an oxidation treatment and during ethylene oxidation. Periodic DFT models allowed assignments of oxygen species detected by *in situ* Raman spectroscopy with detailed structures on p(4 × 4)−O−Ag(111) surfaces. *In situ* NAP-XPS and Raman spectroscopy suggest that $Ag_4{-}O_2$ on oxidized Ag is the active oxygen species for ethylene epoxidation. The experimental and theoretical methodologies developed in the present work serve as an efficient toolbox for the scientific investigation of the silver−oxygen system for selective oxidation reactions and rational guidance of computational calculations coupled with experimental findings.

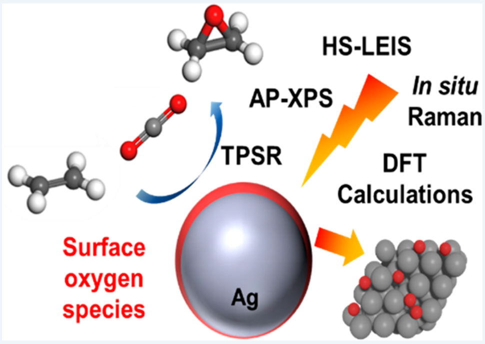

KEYWORDS: *ethylene, oxidation, ethylene oxide, silver, NAP-XPS, in situ Raman, TPSR, DFT*

Silver catalysts find wide industrial application for ethylene epoxidation to ethylene oxide (EO) because of their unique high EO selectivity for this important chemical reaction.[1,2] Despite decades of research effort, the nature of the active oxygen species on/in silver catalysts is still extensively debated because of the scarcity of characterization studies under reaction conditions and computational studies. Elucidation of the oxygen species on/in model Ag powder catalysts and their reactivity and selectivity with ethylene would allow for a guided rational design of highly selective catalysts for ethylene epoxidation.

Over the years, the oxygen species on/in Ag have been probed with various techniques. X-ray photoelectron spectroscopy (XPS) of oxygen on Ag single crystals detected two types of oxygen species assigned to nucleophilic oxygen (O_{nucl}, 528−528.5 eV) and electrophilic oxygen (O_{elec}, 530−531 eV).[3−6] Both oxygen species were observed to participate in the ethylene epoxidation reaction. Of the two, O_{elec} was assumed to attack the π electrons of ethylene and proposed as the EO selective oxygen species. The oxygen species on/in Ag were also detected with *in situ* Raman spectroscopy. Their assignments have been speculated to be Ag_3O (300 cm^{-1}),[7] $Ag{-}O_{bulk}$ (630 cm^{-1}),[8] $Ag{-}(O{-}O)^{2-}$ (697 cm^{-1}), subsurface Ag−O (802 cm^{-1}),[9] Ag═O (956 cm^{-1}),[10] and molecular $Ag{-}O_2$ (1053, 1078, 1286 cm^{-1}).[11,12] In addition to surface oxygen species, subsurface oxygen is also believed to strongly influence the catalytic properties of Ag.[13,14] A consensus on the oxidation state of silver and nature of the oxygen species and their reactivity, however, has not been reached to date. In this context, density functional theory (DFT) calculations can potentially map Raman spectroscopy bands for the O−Ag system with plausible surface and adsorbate structures.[7,15,16] Recent studies showed examples of such an approach, in which hybrid surface−subsurface O_2* species on fully (Ag_2O(001)) or partially oxidized Ag surfaces (the p(4 × 4) oxidic reconstruction of Ag(111)) were found to exhibit vibrational frequencies between 600 and 840 cm^{-1}.[7,17]

The present investigation examines the nature of the oxygen species on/in silver (high-purity electrolytic polycrystalline powder, 99.9999%, 30−60 mesh, Handy & Harman) and their reactivity by the application of scanning electron microscopy (SEM), quasi *in situ* high-sensitivity−low-energy ion scattering (HS-LEIS) spectroscopy, *in situ* Raman spectroscopy, near-ambient-pressure X-ray photoelectron spectroscopy (NAP-XPS), temperature-programmed surface reaction (TPSR) spectroscopy, and steady-state catalytic studies. Combined density functional theory (DFT) calculations and experimental results suggest that $Ag_4{-}O_2$ on a partially oxidized Ag surface is associated with EO formation.

The SEM images of the oxidized model Ag catalyst (40% O_2, 250 °C) are presented in Figure 1a,b. The Ag particles possess a

Received: December 23, 2021
Revised: February 16, 2022

https://doi.org/10.1021/acscatal.1c05939
ACS Catal. 2022, 12, 4375−4381

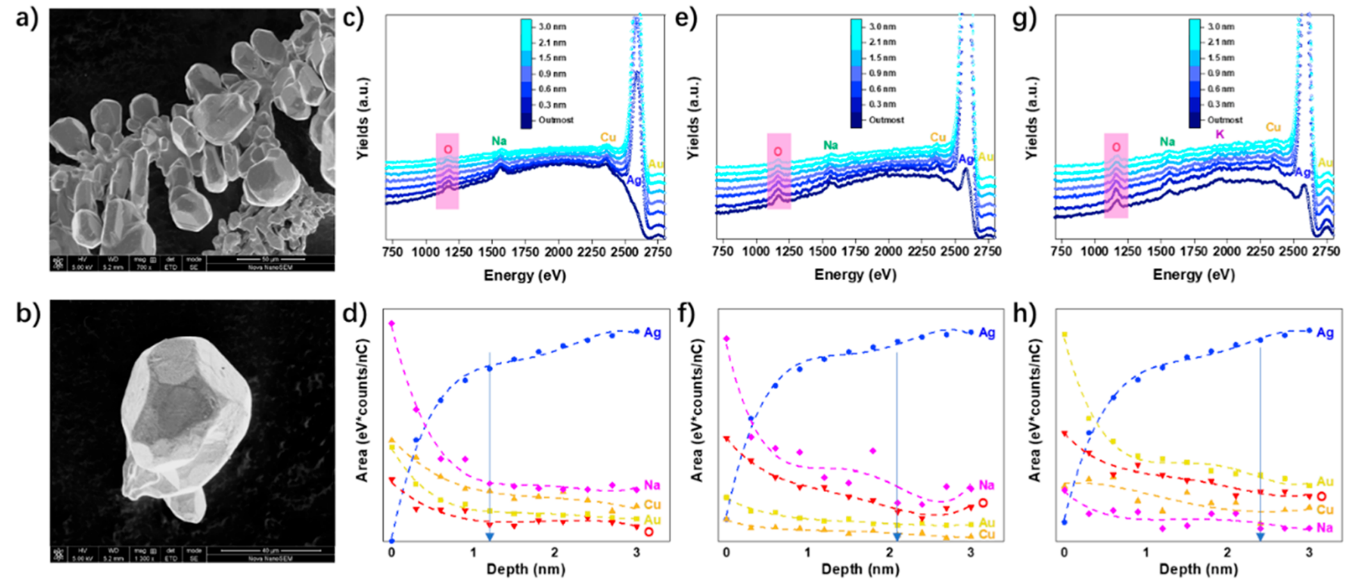

Figure 1. (a) SEM image of the Ag powder after dehydration (Ar at 450 °C) and strong oxidation (40% O_2, 250 °C). (b) SEM image at higher magnification focusing on a single Ag particle. (c) HS-LEIS spectra and (d) depth profile of the Ag catalyst after dehydration (Ar at 450 °C for 1 h). (e) HS-LEIS spectra and (f) depth profile of Ag catalyst after dehydration and mild oxidation (Ar at 450 °C for 1h followed by 5%O_2 at 175 °C for 30 min). (g) HS-LEIS spectra and (h) depth profile of the Ag catalyst after dehydration and strong oxidation (Ar at 450 °C for 1 h followed by 40% O_2 at 250 °C for 30 min).

uniform polyhedral morphology with size ranging from tens to hundreds of micrometers (surface area ~0.01 m^2/g). The atomic composition of the outermost Ag layers was probed by HS-LEIS. The HS-LEIS spectra for the Ag catalyst after dehydration (Ar, 450 °C, 1 h) and mild oxidation (175 °C, 5% O_2, 30 min) and strong oxidation (250 °C, 40% O_2, 30 min) annealing (see schematic in Figure S1) are presented in Figure 1c/d,e/f,g/h, respectively. Despite the extremely high bulk purity, the outmost surface layer of the Ag catalyst contains Cu and Au that are believed to be left over from the Ag purification process, as well as the common impurities of Na, K, and As that may also be related to the manufacturing process. The Au, Cu, Na, and K species are surface-enriched since their HS-LEIS signals decrease with sputtering depth. Upon sputtering, the Ag signal continuously increases while the O signal continuously decreases, reflecting the surface enrichment of O, indicating that the surface of the Ag catalyst is covered by a thin oxide layer. Upon annealing in Ar at 450 °C for 1 h, the surface of the Ag catalyst becomes dehydrated and bulk oxygen is desorbed. The integrated areas of the HS-LEIS signals versus sputtering depth are plotted in Figure 1d,f,h for the Ag surface after dehydration, mild oxidation, and strong oxidation treatments, respectively. Some O species remain in the outermost three layers after dehydration. Examining the relative sensitivity factor (RSF) normalized analysis of O/metal signals (Figure S2), reveals that (i) the surface O concentration is related to the treatment temperature with more surface O segregation as the temperature increases and (ii) the oxide layer increases with the strength of the oxidative pretreatment (~1 nm after dehydration, ~2 nm after mild oxidation, and ~2−3 nm after strong oxidation). The surface of the Ag particles was also found to be nonuniform and is discussed in detail at the beginning of the Supporting Information.

Plane wave periodic DFT calculations were employed to compute the adsorption structures, binding energies, and vibrational frequencies of surface atomic (O*) and surface molecular (O_2*) species on the various Ag silver facets (Figure S3) (111), (110), (100), and (211) and the oxygen-reconstructed surfaces, viz. the p(4 × 4) oxidic reconstruction of the Ag(111) surface (Figure 2).[18,19] The adsorption modes

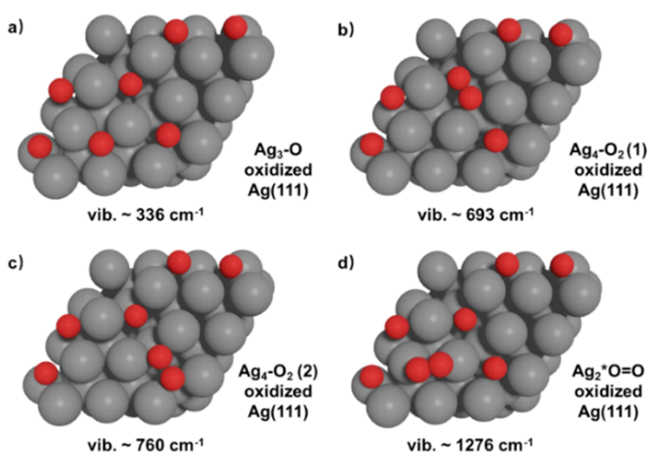

Figure 2. Optimized DFT models on the partially oxidized Ag(111) facet of (a) Ag_3−O with vibration at ~336 cm^{-1}, (b) O−O vibration of Ag_4−O_2 with vibration at ~693 cm^{-1}, (c) O−O vibration on Ag_4−O_2 with vibration at ~760 cm^{-1} ,and (d) Ag_2*O═O with vibration at ~1276 cm^{-1}. Silver atoms are shown in gray; O atoms are shown in red.

and vibrational frequencies are reported in Table 1 and, where possible, compared with those in the literature. The list of DFT-simulated adsorbed oxygen structures can be generally divided into three regions on the basis of their vibrational frequencies: (i) surface O* species exhibiting Ag−O vibrations in the 300−500 cm^{-1} range with Ag−O_{bulk} species also vibrating in the same range (Figure S19 and Table 1), (ii) surface O_2* dioxygen species on Ag exhibiting O−O vibrations in the 600−800 cm^{-1} range (Ag_4−O−O), and (iii) surface molecular O_2* species on Ag exhibiting O═O vibrations in the 1000−1200 cm^{-1} range (Ag_2*O═O). The relations between binding energies and

https://doi.org/10.1021/acscatal.1c05939
ACS Catal. 2022, 12, 4375−4381

Table 1. Simulated Vibrational Frequencies of Oxygen Species on Various Ag Facets in This Study and the Literature

species	facet	site	vibrational frequency (cm^{-1}) this study	literature
Ag_3−O	Ag(111)	FCC 3-fold	351	352[32]
Ag_3−O	Ag(110)	4-fold	*301*	328[33]
Ag_3−O	Ag(100)	4-fold	293	241[34]
Ag_3−O	oxidized Ag(111)	FCC 3-fold	*336*	
Ag−O in Ag_4−O_2	oxidized Ag(111)	trough	362	
O−Ag−O	Ag_2O(001)	bulk	449	
added-row O	p(2 × 1)−O−Ag(110)	added-row	*531*	589[34]
Ag_4−O_2	Ag(110)	4-fold	*751*	753[35]
Ag_4−O_2	Ag(100)	4-fold	788	782[35]
Ag_4−O_2	oxidized Ag(111)	trough	*693*, 760	
Ag_2−*O═O	Ag(111)	bridge	1122	1149[35]
Ag_2−*O═O	oxidized Ag(111)	FCC 3-fold	1276	

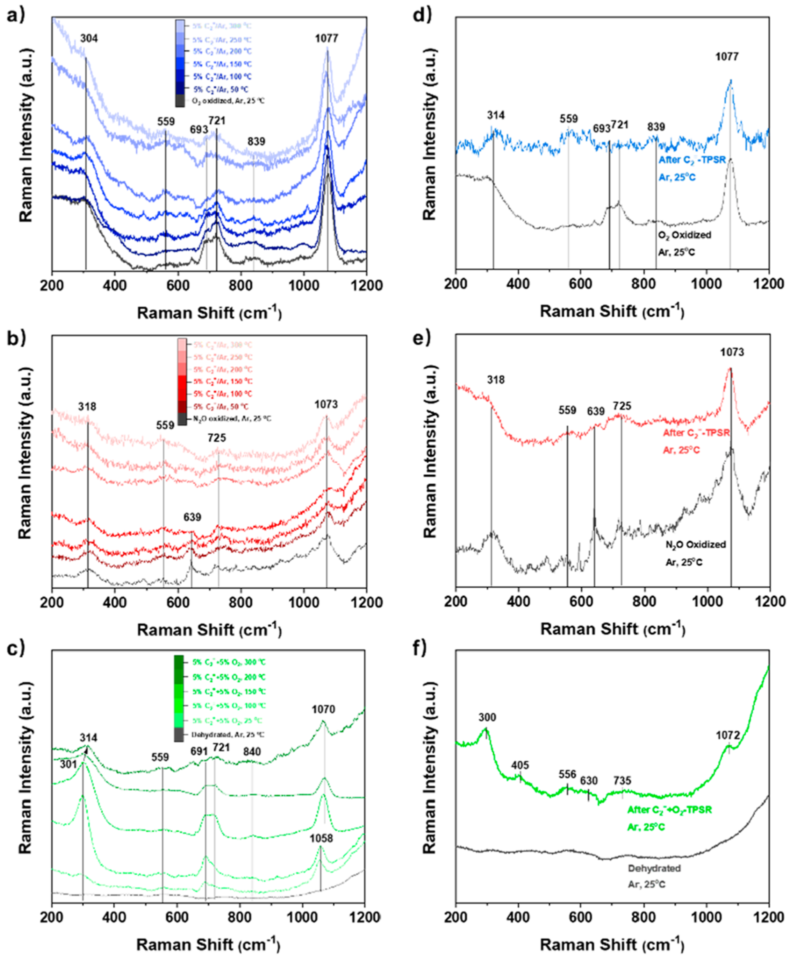

Figure 3. *In situ* Raman spectra of the model Ag catalyst during (a) 5% $C_2^=$-TPSR after oxidation with 40% O_2 (250 °C), (b) 5% $C_2^=$-TPSR after oxidation with 10% N_2O (250 °C), and (c) 5% $C_2^=$ + 5% O_2 -TPSR after dehydration treatment with Ar (450 °C). Comparison of *in situ* Raman spectra of model Ag catalyst (d) after 5% $C_2^=$-TPSR and 40% O_2 oxidized Ag under flowing Ar at room temperature, (e) after 5% $C_2^=$- TPSR and 10% N_2O oxidized Ag in Ar at room temperature, and (f) after 5% $C_2^=$ + 5% O_2-TPSR from 25−300 °C and dehydration with Ar at room temperature.

calculated vibrations of all calculated Ag_x−O species are shown in Figure S4 and Table S1.

The structure and reactivity of various oxygen species toward ethylene oxidation were examined with *in situ* Raman spectroscopy. The local surface roughness of the electrolytic Ag powder gives rise to the surface-enhanced Raman scattering (SERS) effect that enhances the Raman signal intensity by orders of magnitude, thus overcoming the extremely weak surface signals typically associated with very-low-surface-area materials.[20] The *in situ* Raman spectra of the model Ag catalyst after oxidation treatments at 250 °C with O_2 and N_2O, as well as under ethylene oxidation, are exhibited in Figures 3a−c, respectively. A total of six different Raman bands at ca. 304, 559, 639, 691, 721, 839, and 1060−1078 cm^{-1} were detected (Table 2). The 1060−1078

https://doi.org/10.1021/acscatal.1c05939
ACS Catal. 2022, 12, 4375−4381

Table 2. Assignments and Reactivity of Oxygen Species Observed during *In Situ* Raman Spectroscopy Studies

Raman shift (cm^{-1})[a]	oxygen species	reactivity with ethylene	ref
304, *314*, *318*	Ag_3−O	react at 150−300 °C, partially remained after $C_2^=$-TPSR at 300 °C	Figure S19, 10
559	added-row O	unclear due to spatial heterogeneity	34, 36
639	added-row O	react at 50−150 °C, fully consumed upon reaction with $C_2^=$	34
691, *721*	Ag_4−O_2	react at 150−300 °C, fully consumed upon reaction with $C_2^=$	11
839, 840	Ag_4−O_2	unclear due to spatial heterogeneity	11
1060−1078	Na_2CO_3	stable upon exposure to $C_2^=$ up to 300 °C	Figure S5

[a]Italicized Raman shifts exhibit the best agreements with those of italicized shifts from DFT calculations in Table 1.

cm^{-1} band arises from the presence of Na_2CO_3 nanoparticles (see Figure S5). None of these bands were related to surface nitrate species (potential impurity from catalyst synthesis with bands at 1030 and 1258 cm^{-1}; see Figures S6−S8) and adsorbed $^*O_3$ species (Ag−O_3, band at 1165 cm^{-1}; see Figure S9).

The DFT results suggest that the vibrational modes at around 800 cm^{-1} can be attributed to molecular O_2* species confined in the troughs of the p(4 × 4) oxidic reconstruction of the Ag(111) surface (Figure 2b,c). Although similar vibrations were also found in 4-fold sites of *nonreconstructed* metallic surfaces (Figure S3b,c) of more open facets such as Ag(110) and Ag(100), *ab initio* atomistic thermodynamic phase diagram studies[20] show that oxidic reconstructions of the Ag(111) and Ag(110) facets are more stable in comparison to their nonreconstructed metallic counterparts under reaction conditions that are relevant to ethylene oxidation. The vibration range of calculated Ag_4−O_2 species (700−800 cm^{-1}) exhibits good agreement with the hybrid oxygen species (600−810 cm^{-1}) reported in the recent literature.[7] In comparing the binding energies with the vibrational frequencies of the surface O* and O_2* species on both oxygen reconstructed and pristine metallic facets (Figure S4), an intuitive general trend is observed. Surface O_2* species with binding energies larger than that of O_2* on Ag(111) exhibit O−O vibrations at wavenumbers lower than 800 cm^{-1}, as the strong O−Ag bond lowers the O−O bond strength. Surface O* species with binding energies larger than that of O* on Ag(111) (1/3 ML) similarly exhibited Ag−O vibrations at wavenumbers lower than 380 cm^{-1}. In addition to the Ag_x-O species identified above, O_2/Ag−O_{sub} species (O_2* adsorbed near a subsurface O atom) (1165 cm^{-1}) and monodentate, bidentate, and tridentate CO_3/NO_3 on Ag(111) have also been calculated and the detailed structures are shown in Figures S6−S12. The spectroscopic assignments of the aforementioned oxygen species have also been previously proposed from isotopic ^{18}O−^{16}O exchange measurements: the band at ∼300 cm^{-1} was assigned to surface atomic Ag_x−O and the bands at ∼700 and ∼840 cm^{-1} were both assigned to surface Ag_x−O_2 dioxygen species.[10,11] Additionally, DFT simulations of O_2* species on metallic Ag facets that contain subsurface O atoms (Figure S4) exhibited a lowering of the binding energy relative to a pristine Ag(111) surface, coupled with an increase in simulated vibrational frequencies (≥1100 cm^{-1}). This includes the proposed O_2/Ag−O_{sub} species with a vibration predicted at ca. 1165 cm^{-1}, which is absent from the *in situ* Raman spectra under all conditions. A recent work by Paolucci et al. similarly attributed the ∼800 cm^{-1} vibration to a nonstandard dioxygen species, although with a different focus on an Ag_2O(001) surface instead of the p(4 × 4) reconstruction in this study.[17] On the basis of the free energy of reaction, the dioxygen species on an Ag_2O(001) surface is more stable than the dioxygen species adsorbed onto an oxygen vacancy on a p(4 × 4) reconstructed surface, although previous phase diagram studies of the Ag(111) surface suggest that the Ag_2O surface is unstable under ethylene epoxidation reaction conditions.[18,21] Nevertheless, the study by Paolucci et al. and this study both suggest that the 800 cm^{-1} species may be a result of a dioxygen species occupying a surface vacancy site created from the removal of a surface atomic oxygen of an oxidized surface. Additionally, the atomic vacancy need not involve direct desorption (e.g., as molecular oxygen): for example, the oxidation of ethylene by a surface O* (resulting in a vacancy and ethylene oxide or acetaldehyde) is thermodynamically favorable, an observation that is in concurrence with the literature.[22]

The *in situ* Raman spectra during $C_2^=$-TPSR are presented in Figure 3a,b. Upon oxidation with molecular O_2, the Ag surface exhibits Raman bands at 691, 721, and 839 cm^{-1} from Ag_4−O_2 dioxygen species. The surface dioxygen species react with ethylene in the 150−250 °C temperature range. Decreasing intensities of the bands at 304 and 559 cm^{-1} also show that surface monatomic Ag_3−O species react with ethylene in the 150−300 °C temperature range. Upon oxidation of the Ag catalyst with N_2O, which decomposes to $N_{2,gas}$ and only deposits atomic surface O* species,[23] only Raman bands at 304, 559, and 639 cm^{-1} are present that primarily correspond to atomic surface O* species. The reactivities of the atomic Ag_3−O species from the oxidation pretreatments by N_2O and O_2 with ethylene during $C_2^=$-TPSR are similar to those on increasing the temperature from 150 to 300 °C. The model Ag catalyst was also probed with *in situ* Raman during the ethylene oxidation reaction (5% $C_2^=$ + 5% O_2), as shown in Figure 3c. During ethylene oxidation, the Raman bands at 691 and 721 cm^{-1} gradually reached a maximum between 100 and 150 °C. From 200 to 300 °C, the intensity of the 691 and 721 cm^{-1} bands decreased, suggesting that surface Ag−O_2 dioxygen species were being consumed. Meanwhile, the Na_2CO_3 nanoparticles (1060−1078 cm^{-1}) remain relatively stable even at high temperatures. It should be noted that the signal to noise ratio of the Raman spectra dramatically decreased at T > 200 °C, possibly from some loss of surface roughness that decreases the SERS effect.[24] The relative stability of the Na_2CO_3 nanoparticles allowed using the carbonate bands at 1060−1078 cm^{-1} as an internal standard for normalization of the *in situ* Raman spectra.[25] The evolution of the integrated areas of the various oxygen species during *in situ* Raman measurements are presented in Figure S13. To avoid coincidence from surface inhomogeneity and confirm the trend of the observations, Raman spectra were also collected at a second spot and plotted in Figure S14 for reproducibility. After the *in situ* Raman-TPSR experiments, the catalysts were also flushed with Ar and cooled to room temperature and the resulting Raman spectra compared with the spectra of the corresponding oxidized/dehydrated catalysts shown in Figures 3d−f. The surface of the initial dehydrated model Ag catalyst (Figure S15) is found to become oxidized upon exposure to the ethylene oxidation reaction environment (Figure 3f). Raman vibrations from oxidized Cu, Au, and As surface impurities are absent from the Raman spectra (Table S2 and Figure S16) because of the much stronger SERS signal from Ag than from Cu, Au, and As.[26]

https://doi.org/10.1021/acscatal.1c05939
ACS Catal. 2022, 12, 4375−4381

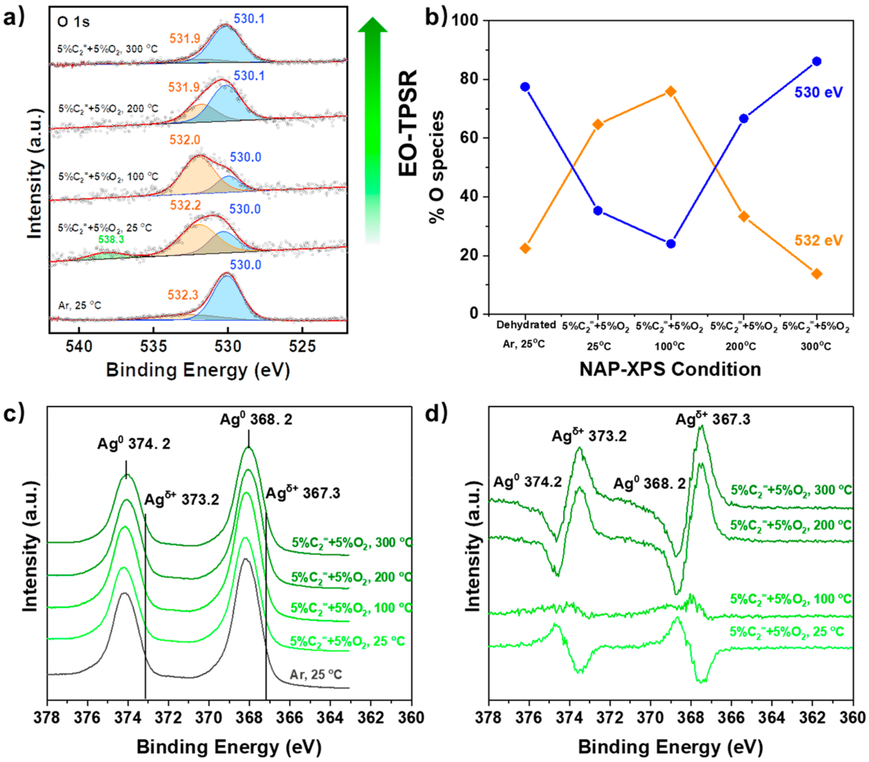

Figure 4. (a) *In situ* NAP-XPS spectra of the O 1s region of model Ag catalysts during ethylene oxidation. (b) Percentage of oxygen species with binding energies of 532 and 530 eV measured under different reaction conditions. (c) *In situ* NAP-XPS spectra of the Ag 3d region of model Ag catalysts during ethylene oxidation. (d) Difference Ag 3d spectra during ethylene oxidation by model Ag catalysts at different temperatures relative to the corresponding spectra of dehydration treatments.

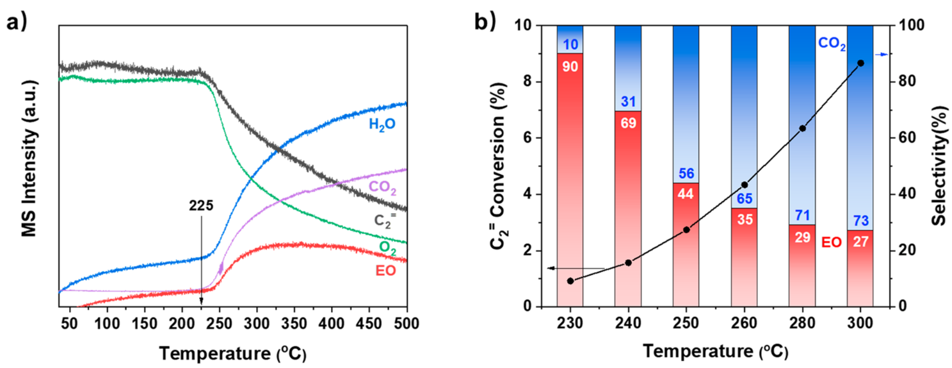

Figure 5. (a) TPSR profile during ethylene oxidation (5% $C_2^=$ + 5% O_2) by the model Ag catalyst from 30 to 500 °C. (b) Steady-state reaction performance for ethylene oxidation (5% $C_2^=$ + 5% O_2) by the model Ag catalyst.

The reaction of ethylene with the oxygen species on/in the model Ag catalyst during the ethylene oxidation reaction (5% $C_2^=$ + 5% O_2) was also monitored with NAP-XPS, and the spectra are presented in Figure 4a. The XPS O 1s peak at a binding energy (BE) of 538.3 eV is from gas-phase molecular O_2. The O 1s peak at a BE of 538.3 eV is only present at 25 °C and is absent at higher temperatures, indicating that it is completely consumed at higher reaction temperatures. The O 1s peaks at BEs of ~530.0 and ~532.0 eV have been assigned in the literature to atomic O_{bulk} species[8,27] and surface Ag_x−O_2 dioxygen species.[28−30] The relative population of the O 1s peaks at 530 eV (O_{bulk}) and 532 eV (surface Ag_x−O_2) as a function of environmental conditions is indicated in Figure 4b. The O_{bulk} peak (530 eV) is the dominant oxygen species after the initial dehydration/O_2 desorption treatment, and its intensity initially decreases and then increases above 100 °C with the reaction temperature. The surface Ag_x−O_2 dioxygen species (532 eV) exhibits an inverse trend, with its intensity initially increasing up to 100 °C and then decreasing with increasing reaction temperature (Figure 4b). The trend of Ag_x−O_2 agrees with the evolution of Raman bands corresponding to Ag_4−O_2 that vibrate at 691−721 cm^{-1} (Figure 3c). The corresponding Ag 3d NAP-XPS spectra presented in Figure 4c indicate that Ag is predominately metallic during ethylene oxidation.[31] The Ag 3d difference spectra (Figure 4d) at various temperatures, however, reveal that the model silver catalyst gradually becomes mildly oxidized during ethylene oxidation, forming $Ag^{\delta+}$ (Ag 3d peaks at 367.3 and 373.2 eV). The increase in the $Ag^{\delta+}$ signal at elevated reaction temperatures further suggests that the surface region (1−3 nm) probed by XPS is

https://doi.org/10.1021/acscatal.1c05939
ACS Catal. 2022, 12, 4375−4381

partially oxidized in the ethylene oxidation reaction. In addition, NAP-XPS of the oxidized Ag powder during $C_2^=$-temperature-programmed surface reaction (TPSR) is shown in Figure S17 and reveals that the surface Ag_x-O_2 species are preferentially consumed during $C_2^=$-TPSR from 50 to 200 °C. The peak deconvolution shown in Figure S18 confirms that the Ag surface is partially oxidized and constitutes 10.98% and 8.76% of $Ag^{\delta+}$ in the oxidative treatment and ethylene oxidation, respectively. The concentration of Ag_x-O_2 species on the oxidized Ag surface is also found to undergo a slight increase (Figure S17b) when the environment is switched from Ar to 5% $C_2^=$ (absence of molecular O_2), suggesting that surface Ag_x-O_2 is being formed from the $Ag-O_{bulk}$ species.

Correlation of the *in situ* Raman spectra and steady-state performance of the model Ag catalyst suggests that surface Ag_4-O_2 is the more selective species for EO formation, as indicated in Figure 5a. The $C_2^=+O_2$-TPSR spectrum shows that the production of EO is initiated at 225 °C and reaches a maximum at ca. 300 °C in conjunction with the formation of CO_2 and water as side products. The MS signal intensities of the CO_2 and water products continue to increase beyond 300 °C while the EO signal no longer increases, which corresponds to the almost complete consumption of the surface Ag_4-O_2 species while Ag_3-O species are still present (Figure 3c,f). A steady-state catalytic evaluation (Figure 5b) also exhibited that the EO selectivity gradually decreases with increasing reaction temperature. Thus, it is suggested that the surface Ag_4-O_2 species are more selective than Ag_3-O for EO formation.

In conclusion, the nature of the surface oxygen species formed on oxidized Ag was determined with the application of quasi *in situ* HS-LEIS spectroscopy, *in situ* Raman spectroscopy, *in situ* NAP-XPS spectroscopy, and DFT calculations. The surface of the Ag powder catalyst is partially oxidized with ~9% $Ag^{\delta+}$ in the ethylene oxidation reaction environment. The detailed structures of Ag_x-O species observed in the Raman spectra were assigned by DFT calculations on the p(4 × 4)−O−Ag(111) surface. The simultaneous preferential consumption of surface Ag_4-O_2 species on partially oxidized Ag and formation of EO during the $C_2H_4 + O_2$ reaction suggests that the surface Ag_4-O_2 species is the more selective oxygen species for EO formation. The present study provides new fundamental insights into the selective oxidation of ethylene by Ag catalysts.

■ ASSOCIATED CONTENT

Supporting Information

The Supporting Information is available free of charge at https://pubs.acs.org/doi/10.1021/acscatal.1c05939.

> Experimental materials and methods, supplementary figures and tables for characterization and DFT calculations, including a schematic illustration of the surface treatment of Ag powder, a depth profile of the RSF plot, *in situ* NAP-XPS spectra, *in situ* Raman spectra, ambient Raman spectra of reference compounds, and DFT models of oxygen, carbonate, and nitrate species on Ag surface, and tables of detailed structure information (PDF)

■ AUTHOR INFORMATION

Corresponding Authors

Israel E. Wachs − *Operando Molecular Spectroscopy & Catalysis Laboratory, Department of Chemical and Biomolecular Engineering, Lehigh University, Bethlehem, Pennsylvania 18015, United States;* orcid.org/0000-0001-5282-128X; Email: iew0@lehigh.edu

Srinivas Rangarajan − *Computational Catalysis and Materials Design Group, Department of Chemical and Biomolecular Engineering, Lehigh University, Bethlehem, Pennsylvania 18015, United States;* orcid.org/0000-0002-6777-9421; Email: srr516@lehigh.edu

Authors

Tiancheng Pu − *Operando Molecular Spectroscopy & Catalysis Laboratory, Department of Chemical and Biomolecular Engineering, Lehigh University, Bethlehem, Pennsylvania 18015, United States;* orcid.org/0000-0002-4775-4294

Adhika Setiawan − *Computational Catalysis and Materials Design Group, Department of Chemical and Biomolecular Engineering, Lehigh University, Bethlehem, Pennsylvania 18015, United States*

Bar Mosevitzky Lis − *Operando Molecular Spectroscopy & Catalysis Laboratory, Department of Chemical and Biomolecular Engineering, Lehigh University, Bethlehem, Pennsylvania 18015, United States*

Minghui Zhu − *State Key Laboratory of Chemical Engineering, East China University of Science and Technology, Shanghai 200237, People's Republic of China;* orcid.org/0000-0003-1593-9320

Michael E. Ford − *Operando Molecular Spectroscopy & Catalysis Laboratory, Department of Chemical and Biomolecular Engineering, Lehigh University, Bethlehem, Pennsylvania 18015, United States;* orcid.org/0000-0002-0403-801X

Complete contact information is available at:
https://pubs.acs.org/10.1021/acscatal.1c05939

Author Contributions

‖T.P., A.S., and B.M.L. contributed equally.

Notes

The authors declare no competing financial interest.

■ ACKNOWLEDGMENTS

Financial support from an NSF GOALI grant (#1804104) and assistance from Dr. Ryan Thorpe with the HS-LEIS measurements are gratefully acknowledged.

■ REFERENCES

(1) Pu, T.; Tian, H.; Ford, M. E.; Rangarajan, S.; Wachs, I. E. Overview of Selective Oxidation of Ethylene to Ethylene Oxide by Ag Catalysts. *ACS Catal.* **2019**, *9*, 10727−10750.

(2) Rebsdat, S.; Mayer, D. Ethylene Oxide. *Ullmann's Encyclopedia of Industrial Chemistry*; Wiley: 2001.

(3) Bukhtiyarov, V. I.; Nizovskii, A. I.; Bluhm, H.; Hävecker, M.; Kleimenov, E.; Knop-Gericke, A.; Schlögl, R. Combined in Situ XPS and PTRMS Study of Ethylene Epoxidation over Silver. *J. Catal.* **2006**, *238*, 260−269.

(4) Rocha, T. C. R.; Hävecker, M.; Knop-Gericke, A.; Schlögl, R. Promoters in Heterogeneous Catalysis: The Role of Cl on Ethylene Epoxidation over Ag. *J. Catal.* **2014**, *312*, 12−16.

(5) Carbonio, E. A.; Rocha, T. C. R.; Klyushin, A. Y.; Píš, I.; Magnano, E.; Nappini, S.; Piccinin, S.; Knop-Gericke, A.; Schlögl, R.; Jones, T. E. Are Multiple Oxygen Species Selective in Ethylene Epoxidation on Silver? *Chem. Sci.* **2018**, *9*, 990−998.

(6) Jones, T. E.; Rocha, T. C. R.; Knop-Gericke, A.; Stampfl, C.; Schlögl, R.; Piccinin, S. Insights into the Electronic Structure of the Oxygen Species Active in Alkene Epoxidation on Silver. *ACS Catal.* **2015**, *5*, 5846−5850.

(7) Tang, Z.; Chen, T.; Liu, K.; Du, H.; Podkolzin, S. G. Atomic, Molecular and Hybrid Oxygen Structures on Silver. *Langmuir* **2021**, *37*, 11603−11610.

(8) Bao, X.; Muhler, M.; Pettinger, B.; Schlögl, R.; Ertl, G. On the Nature of the Active State of Silver during Catalytic Oxidation of Methanol. *Catal. Lett.* **1993**, *22*, 215−225.

(9) Bao, X.; Pettinger, B.; Ertl, G.; Schlogl, R. In-Situ Raman Studies of Ethylene Oxidation at Ag(111) and Ag(110) under Catalytic Reaction Conditions. *Berichte der Bunsengesellschaft/Physical Chem. Chem. Phys.* **1993**, *97*, 322−325.

(10) Wang, C.-B.; Deo, G.; Wachs, I. E. Interaction of Polycrystalline Silver with Oxygen, Water, Carbon Dioxide, Ethylene, and Methanol: In Situ Raman and Catalytic Studies. *J. Phys. Chem. B* **1999**, *103*, 5645−5656.

(11) Pettenkofer, C.; Pockrand, I.; Otto, A. Surface Enhanced Raman Spectra of Oxygen Adsorbed on Silver. *Surf. Sci.* **1983**, *135*, 52−64.

(12) Tevault, D. E.; Smardzewski, R. R.; Urban, M. W.; Nakamoto, K. Catalytic Intermediates in the Ag-O2 System. Evidence for a Nonsymmetric AgO2Molecule. *J. Chem. Phys.* **1982**, *73*, 5500.

(13) Xu, Y.; Greeley, J.; Mavrikakis, M. Effect of Subsurface Oxygen on the Reactivity of the Ag(111) Surface. *J. Am. Chem. Soc.* **2005**, *127*, 12823−12827.

(14) Michaelides, A.; Bocquet, M. L.; Sautet, P.; Alavi, A.; King, D. A. Structures and Thermodynamic Phase Transitions for Oxygen and Silver Oxide Phases on Ag{1 1 1}. *Chem. Phys. Lett.* **2003**, *367*, 344−350.

(15) Linic, S.; Barteau, M. A. Formation of a Stable Surface Oxametallacycle That Produces Ethylene Oxide. *J. Am. Chem. Soc.* **2002**, *124*, 310−317.

(16) Huš, M.; Hellman, A. Ethylene Epoxidation on Ag(100), Ag(110), and Ag(111): A Joint Ab Initio and Kinetic Monte Carlo Study and Comparison with Experiments. *ACS Catal.* **2019**, *9*, 1183−1196.

(17) Liu, C.; Wijewardena, D. P.; Sviripa, A.; Flaherty, D. W.; Paolucci, C. Computational and Experimental Insights into Reactive Forms of Oxygen Species on Dynamic Ag Surfaces under Ethylene Epoxidation Conditions. *J. Catal.* **2021**, *405*, 445−461.

(18) Martin, N. M.; Klacar, S.; Grönbeck, H.; Knudsen, J.; Schnadt, J.; Blomberg, S.; Gustafson, J.; Lundgren, E. High-Coverage Oxygen-Induced Surface Structures on Ag(111). *J. Phys. Chem. C* **2014**, *118*, 15324−15331.

(19) Schnadt, J.; Knudsen, J.; Hu, X. L.; Michaelides, A.; Vang, R. T.; Reuter, K.; Li, Z.; Lãægsgaard, E.; Scheffler, M.; Besenbacher, F. Experimental and Theoretical Study of Oxygen Adsorption Structures on Ag(111). *Phys. Rev. B - Condens. Matter Mater. Phys.* **2009**, *80*, 075424.

(20) Hess, C. New Advances in Using Raman Spectroscopy for the Characterization of Catalysts and Catalytic Reactions. *Chem. Soc. Rev.* **2021**, *50*, 3519−3564.

(21) Jones, T. E.; Rocha, T. C. R.; Knop-Gericke, A.; Stampfl, C.; Schlögl, R.; Piccinin, S. Thermodynamic and Spectroscopic Properties of Oxygen on Silver under an Oxygen Atmosphere. *Phys. Chem. Chem. Phys.* **2015**, *17*, 9288−9312.

(22) Jones, T. E.; Wyrwich, R.; Bocklein, S.; Rocha, T. C. R.; Carbonio, E. A.; Knop-Gericke, A.; Schlogl, R.; Gunther, S.; Wintterlin, J.; Piccinin, S. Oxidation of Ethylene on Oxygen Reconstructed Silver Surfaces. *J. Phys. Chem. C* **2016**, *120*, 28630−28638.

(23) Chen, C. J.; Harris, J. W.; Bhan, A. Kinetics of Ethylene Epoxidation on a Promoted Ag/α-Al2O3 Catalyst—The Effects of Product and Chloride Co-Feeds on Rates and Selectivity. *Chem. - A Eur. J.* **2018**, *24*, 12405−12415.

(24) Pockrand, I.; Otto, A. Surface Enhanced Raman Scattering (SERS): Annealing the Silver Substrate. *Solid State Commun.* **1981**, *38*, 1159−1163.

(25) Isegawa, K.; Ueda, K.; Amemiya, K.; Mase, K.; Kondoh, H. Formation and Behavior of Carbonates on Ag(110) in the Presence of Ethylene and Oxygen. *J. Phys. Chem. C* **2021**, *125*, 9032−9037.

(26) Le Ru, E. C.; Blackie, E.; Meyer, M.; Etchegoint, P. G. Surface Enhanced Raman Scattering Enhancement Factors: A Comprehensive Study. *J. Phys. Chem. C* **2007**, *111*, 13794−13803.

(27) Dupin, J. C.; Gonbeau, D.; Vinatier, P.; Levasseur, A. Systematic XPS Studies of Metal Oxides, Hydroxides and Peroxides. *Phys. Chem. Chem. Phys.* **2000**, *2*, 1319−1324.

(28) Au, C. T.; Singh-Boparai, S.; Roberts, M. W.; Joyner, R. W. Chemisorption of Oxygen at Ag(110) Surfaces and Its Role in Adsorbate Activation. *J. Chem. Soc. Faraday Trans. 1 Phys. Chem. Condens. Phases* **1983**, *79*, 1779−1791.

(29) Boronin, A. I.; Koscheev, S. V.; Malakhov, V. F.; Zhidomirov, G. M. Study of High-Temperature Oxygen States on the Silver Surface by XPS and UPS. *Catal. Lett.* **1997**, *47*, 111−117.

(30) Boronin, A. I.; Koscheev, S. V.; Murzakhmetov, K. T.; Avdeev, V. I.; Zhidomirov, G. M. Associative Oxygen Species on the Oxidized Silver Surface Formed under O2Microwave Excitation. *Appl. Surf. Sci.* **2000**, *165*, 9−14.

(31) Karatok, M.; Sensoy, M. G.; Vovk, E. I.; Ustunel, H.; Toffoli, D.; Ozensoy, E. Formaldehyde Selectivity in Methanol Partial Oxidation on Silver:Effect of Reactive Oxygen Species, Surface Reconstruction, and Stability of Intermediates. *ACS Catal.* **2021**, *11*, 6200−6209.

(32) Chen, B. W. J.; Kirvassilis, D.; Bai, Y.; Mavrikakis, M. Atomic and Molecular Adsorption on Ag(111). *J. Phys. Chem. C* **2019**, *123*, 7551−7566.

(33) Stietz, F.; Elbe, A.; Meister, G.; Schaefer, J. A.; Goldmann, A. Submonolayer Coadsorption of Chlorine and Oxygen on Ag(110) Studied by Electron Energy Loss Vibrational Spectroscopy. *J. Phys.: Condens. Matter* **1996**, *8*, 7699−7709.

(34) Bonini, N.; Kokalj, A.; Dal Corso, A.; De Gironcoli, S.; Baroni, S. Structure and Dynamics of Oxygen Adsorbed on Ag(100) Vicinal Surfaces. *Phys. Rev. B - Condens. Matter Mater. Phys.* **2004**, *69*, 1−12.

(35) Montemore, M. M.; Van Spronsen, M. A.; Madix, R. J.; Friend, C. M. O2 Activation by Metal Surfaces: Implications for Bonding and Reactivity on Heterogeneous Catalysts. *Chem. Rev.* **2018**, *118*, 2816−2862.

(36) Pettinger, B.; Bao, X.; Wilcock, I.; Muhler, M.; Schlögl, R.; Ertl, G. Thermal Decomposition of Silver Oxide Monitored by Raman Spectroscopy: From AgO Units to Oxygen Atoms Chemisorbed on the Silver Surface. *Angew. Chem., Int. Ed. Engl.* **1994**, *33*, 85−86.